A&A 366, 121–128 (2001)
DOI: 10.1051/0004-6361:20000193

Astronomy & Astrophysics

Optical variability of the B-type star HD 105382: Pulsation or rotation?*

M. Briquet[1], C. Aerts[2,**], and P. De Cat[2]

[1] Institut d'Astrophysique et de Géophysique de Liège, Université de Liège, avenue de Cointe 5, 4000 Liège, Belgium
[2] Instituut voor Sterrenkunde, Katholieke Universiteit Leuven, Celestijnenlaan 200 B, 3001 Heverlee, Belgium

Received 18 May 2000 / Accepted 26 October 2000

Abstract. We present ground-based multi-colour Geneva photometry and high-resolution high S/N spectra of the variable B-type star HD 105382. We provide evidence that this star is not a Be star, as indicated in the literature. The monoperiodic variability found in the Hipparcos data is confirmed in our ground-based follow-up observations. All existing data give rise to the detection of the period of 1.295 days. We try to interpret the variability of the star in terms of a non-radial g-mode pulsation model and of a rotational modulation model. None of these two is able to explain the observed line-profile variations in full detail.

Key words. stars: early-type – stars: variables: general – stars: oscillations – stars: individual: HD 105382

1. Introduction

In the framework of a long-term photometric and spectroscopic monitoring programme of bright southern Slowly Pulsating B stars (SPBs, see Aerts et al. 1999b) we have at our disposal Geneva photometric and spectroscopic data of the star HD 105382. From the Hipparcos mission it was concluded that this bright star is a B-type variable with only one clear intrinsic period of 1.295 days, which is a period expected for SPBs. Based on the Hipparcos photometry, we would have classified the star as an SPB if it were not for the fact that HD 105382 is listed as a B 6 III e eruptive star in Simbad. Because of the lack of comprehension of strictly periodic Be stars we felt it was important to analyse this variable and compare our result with those obtained for SPBs (of which the first results can be found in Aerts et al. 1999b; De Cat et al. 2000).

Some researchers allocate the cause of periodic light and line-profile variations of Be stars to non-radial pulsation (hereafter termed NRP) while others advocate a rotational modulation model (see Baade & Balona 1994). The interpretation of the discs around Be stars in terms of being caused by the beating of non-radial pulsation modes gained support thanks to the recent study of the Be star μ Cen. Rivinius et al. (1998) were able to show in a very convincing way that the different frequencies found in their numerous spectra obtained over some years give rise to a positive interference, which occurs at the same epochs of the outbursts found in this star. On the other hand, many periodic Be stars are monoperiodic (Balona 1995) and so the beating phenomenon cannot be called upon in such cases to explain disc formation. Balona (1995) interprets the periods in the Be stars in terms of the rotational periods of the stars, mainly based on statistical arguments.

The example of the analyses of high-quality line-profile variations of the Be star 28 CMa shows how difficult it is to derive a correct interpretation of the data. Balona et al. (1999) have interpreted the observed variations in terms of a spot model, while Maintz et al. (2000) were able to produce a successful pulsation model to explain the data. At present there is no consensus about the best model. The only way to proceed in this matter seems to be to increase the number of objects for which high-resolution spectroscopic data are available. Since the photometric variability found in the Hipparcos data of HD 105382 points towards a "simple" variability pattern, we regarded HD 105382 as a perfect test case to study the optical variation of a Be star. Consequently we have included this star in an extensive study mainly devoted to SPBs (Aerts et al. 1999b).

In this paper we envisage the optimum NRP and rotational modulation models to conclude on the best explanation for the origin of the periodic variability in the selected star. The plan of the paper is the following. In Sect. 2 we disprove the Be nature of the star and we

Send offprint requests to: M. Briquet,
e-mail: briquet@astro.ulg.ac.be

* Based on observations obtained with the Swiss photometric telescope and ESO's CAT/CES telescope, both situated at La Silla, Chile.

** Postdoctoral Fellow, Fund for Scientific Research, Flanders.

derive some physical parameters of the star. In Sect. 3 we give the results of the frequency analysis on the Hipparcos photometric data, the Geneva photometric data and the spectroscopic data. Once the frequency analysis is done, we consider a NRP model and make a mode identification from the photometric and spectroscopic data (Sect. 4). Afterwards we envisage a rotational modulation model (Sect. 5). The outcome of the modelling of the line-profile variations of the star is discussed in Sect. 6.

2. HD 105382

Different opinions about the Be character of HD 105382 are present in the literature. The star was classified as a Be star by Hiltner et al. (1969), who found clear emission in the Balmer lines. On the other hand, Dachs et al. (1981) took spectrograms in 1978 and concluded that the star should be deleted from all Be catalogues. Next, Aerts (2000) reports a clear broad Hα emission profile, which shows double-peaked emission with a maximum of 7.5 continuum units observed in May 1996. Rivinius (private communication) pointed out to us that the Hα spectrum shown in Aerts (2000) is very alike the one he took in May 1996 of the B 2 IV e star δ Cen, who is situated only a few arcminutes away from HD 105382. Moreover, he found HD 105382 to exhibit absorption in Hα in January 2000. Because of these contradictions, we have subsequently taken several high-resolution Hα spectra during two weeks in February 2000, all of which are narrow and show absorption. We note that all our data taken for HD 105382 were obtained by remote central from Garching, so that the observer has only a very limited view of the sky.

Other authors also disprove the Be nature of the star. Slettebak et al. (1975) found that no emission is visible in April 1974 and that the spectral type (B 2 III ne) by Hiltner et al. (1969) appears to be too early. We note that this spectral type is the one of δ Cen. Claria et al. (1981) obtained Hα and Hβ observations of a group of normal B and Be stars, among which HD 105382. The values for Hβ that we found in the literature have an average value of 2.68, which points towards a normal B star for its spectral type B 6 III. We therefore conclude that HD 105382 was confused several times with δ Cen and that it is not a Be star. The most likely explanation for the variability therefore seems to be pulsations in terms of high-order g-modes, as these occur in many SPBs in that part of the HR diagram (see Waelkens et al. 1998).

The effective temperature and the gravity of HD 105382 are obtained by means of the photometric calibration by Künzli et al. (1997) to the mean magnitudes in the Geneva filters. The parallax measured by Hipparcos provides the distance. This, together with the average visual magnitude, gives the absolute visual magnitude. One obtains the bolometric magnitude and consequently the luminosity taking into account the bolometric correction (BC), which is calculated by means of the Flower's relation (1996) between $T_{\rm eff}$ and BC. With the values for the effective temperature and the luminosity one estimates the mass by using the evolutionary tracks published by Schaller et al. (1992). We also calculated the radius. The results are:

$$\left\{\begin{array}{l}\log T_{\rm eff} = 4.24 \pm 0.01,\\ \log g = 4.18 \pm 0.15,\\ \log L/L_{\odot} = 2.89 \pm 0.15,\\ M = 5.7\ M_{\odot},\\ R = 3\ R_{\odot}.\end{array}\right.$$

With these parameters, HD 105382 is situated in the upper and blue part of the SPB instability domain (see e.g. Pamyatnykh 1999).

3. Frequency analysis

We performed a frequency analysis on the photometric and spectroscopic data by means of the PDM method (Stellingwerf 1978) and the CLEAN method (Roberts et al. 1987).

3.1. The Hipparcos photometric data

The satellite Hipparcos made 172 useful measurements of HD 105382 spread over a little more than 3 years. We tested frequencies from 0 to 3 cycles per day (c/d) with a frequency step of 0.00001 c/d. The Θ-statistic is represented in Fig. 1. The frequency which corresponds to the minimum of Θ is 0.77213 c/d. A phase diagram with this frequency, fitted with a least-squares sine fit, is shown in Fig. 2. This frequency explains a fraction of the variance of about 86%. Once we had found a significant frequency we searched for an additional frequency. To do so, we subtracted the sine fit from the measurements (i.e. we prewhitened the data with the significant frequency) in order to apply the PDM method on the residuals. As we obtained a variance of the residuals comparable with the mean error of the measurements we could not find another frequency.

3.2. The Geneva photometric data

Measurements of HD 105382 in the Geneva seven colour photometric system were obtained in 1997. These data also reveal the frequency 0.77214 c/d. A phase diagram with this frequency for the filter U is shown in Fig. 3. Again we do not find an additional frequency. In Table 1 we give the amplitudes obtained with a sine fit for the separate filters together with the mean magnitudes in the different filters.

3.3. The spectroscopic data

We have 105 spectra obtained with the CAT/CES during 10 separate weeks of monitoring spread over 1996–1998. We extracted the measurements of the doublet Si II centered at $\lambda\lambda$ 4128, 4130 Å. From these spectral lines we

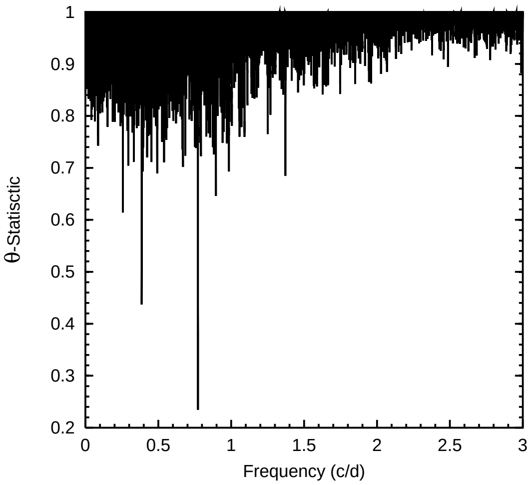

Fig. 1. Θ-Statistic of the Hipparcos photometric data

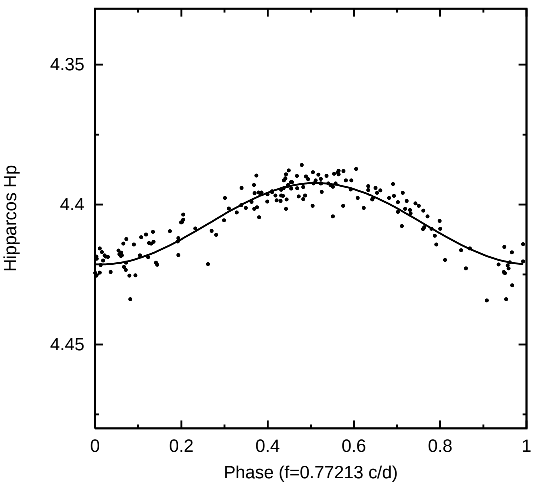

Fig. 2. Phase diagram of the Hipparcos photometric data

computed the radial velocity with the aim of performing a frequency analysis. For each of the lines we found subsequently $f = 0.7721$ c/d, $2f$ and $3f$. The outcome of the CLEAN method for the different steps of the frequency

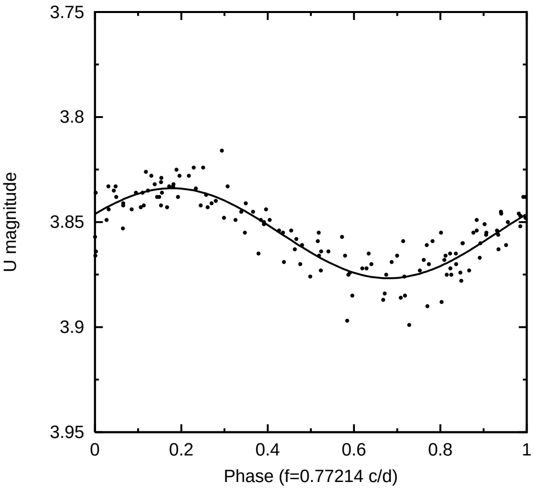

Fig. 3. Phase diagram of the U-magnitude data

Table 1. Amplitudes of the least-squares sine fits to the Geneva data and mean magnitudes in the different filters

Filter	Amplitude	Mean magnitude
U	0.0204 ± 0.0013	3.8553 ± 0.0009
B_1	0.0153 ± 0.0010	4.0896 ± 0.0007
B	0.0145 ± 0.0009	3.2915 ± 0.0007
B_2	0.0141 ± 0.0009	4.8741 ± 0.0006
V_1	0.0120 ± 0.0007	5.1390 ± 0.0005
V	0.0115 ± 0.0007	4.4525 ± 0.0005
G	0.0117 ± 0.0008	5.6716 ± 0.0006

search on the radial velocity of the Si II 4128 Å line is represented in Fig. 4. After prewhitening with f, $2f$, $3f$, no periodicity is present any more in the data.

4. Non-radial pulsation model

In order to confront the observations with a NRP model we have to make a mode identification. To this end we used the method of photometric amplitudes, the moment method and a line-profile fitting technique. In the following sections these methods are briefly described. For a full description of the techniques we refer to Heynderickx et al. (1994), Aerts (1996) and Townsend (1997).

4.1. The Geneva photometric data

The photometric amplitudes of the observed variations depend on the wavelength of the radiation. The theoretical photometric amplitude of a non-rotating pulsating star is a function of the wavelength, the degree ℓ of the pulsation mode and a free parameter $S(S \in [0, 1]$, 0: fully non-adiabatic, 1: adiabatic) taking into account non-adiabatic effects. We note that the parameter S is the same as the parameter R of Stamford & Watson (1981). So we can determine the degree of the pulsation mode by comparing the observed amplitudes at some wavelengths (i.e. those of the central wavelengths of the passbands of the used photometric system) with the theoretical amplitudes calculated for several values of ℓ and S. A brief description of the used method is given in Aerts et al. (1999a).

We can also define a criterion allowing us to determine the most likely mode and to adopt the parameter S by considering the difference between the observed and theoretical amplitudes. This quantity is named the "amplitude difference" and is the lowest for the most likely mode. In Fig. 5 it is calculated as a function of S for $\ell = 0$ to 7. The most likely modes correspond to $\ell = 4$, $\ell = 6$, $\ell = 2$, $\ell = 1$.

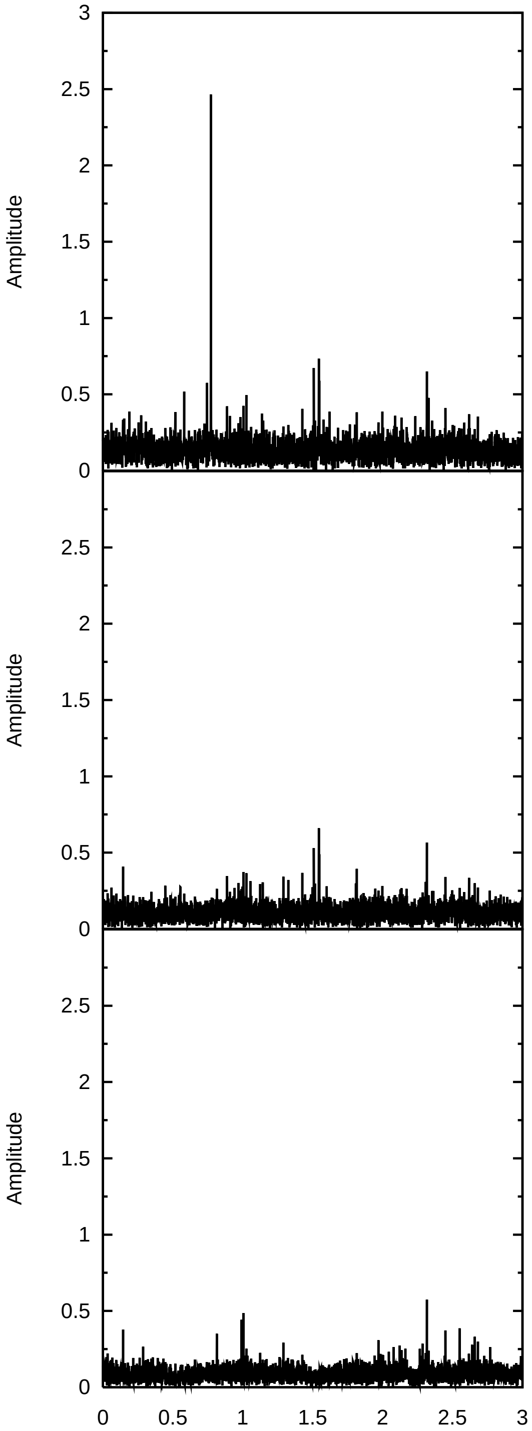

Fig. 4. Outcome of the CLEAN method to the radial velocity derived from the Si II 4128 Å line, to the data prewhitened with f, to the data prewhitened with $2f$

To compute the theoretical photometric amplitude we need $\log T_{\mathrm{eff}}$ and $\log g$, which have been calculated in a previous section. We also need the pulsation constant Q:

$$Q = P\sqrt{\frac{\bar{\rho}}{\bar{\rho}_\odot}},$$

where P is the pulsation period and $\bar{\rho}$ the mean mass density. With the values found for the frequency, the mass and the radius, we obtained $Q = 0.59$. This Q-value and the period clearly indicate that a g-mode is active in the case that the periodicity is due to pulsation.

In Fig. 5 we find the observed amplitude ratios for the Geneva filters together with the curves representing the theoretical amplitudes for the four best solutions. The error bars, which take into account the uncertainty of the derived amplitudes, are also indicated. We note that the amplitudes for the B_1, B, B_2-filters are too large for all the models, while the amplitude for the V-filter is too small. The curve with $\ell = 4$ best fits the observations, but the solutions for $\ell = 1$, 2, 6 are almost equivalent in quality.

We conclude that the photometric behaviour is difficult to model in terms of a linear non-radial pulsation model. We notice that such a model in general does describe the observed amplitudes of β Cep stars and SPBs in an accurate way (see e.g. Heynderickx et al. 1994).

4.2. The spectroscopic data

In order to calculate theoretical line-profile variations that result from NRP, we need to make some assumptions. In this paper, we first adopt a Gaussian intrinsic profile, which is described by $I = I_0 \exp(\triangle\lambda^2/2\sigma^2)$. To adopt the linear limb-darkening coefficient u we used the tabulation of linear limb-darkening data by Wade & Rucinski (1985), which is based on the model atmosphere grid of Kurucz (1979). For T_{eff} and $\log g$ obtained in a previous section we found $u = 0.36$ for the Si II 4128 Å line.

4.2.1. Mode identification by the moment method

To begin we determined the first three moments $\langle v^1\rangle$, $\langle v^2\rangle$ and $\langle v^3\rangle$ of HD 105382 and compared them with theoretical predictions (see e.g. Aerts et al. 1992). The first three moments contain sufficient information to accurately describe a line profile, so we limit to them. Consider the case of a monoperiodic pulsator and a linear pulsation theory. In the slow-rotation approximation, if f is the pulsation frequency, then the theoretical expression of $\langle v^1\rangle$ varies with f, $\langle v^2\rangle$ is represented by a constant term plus two terms varying respectively with f and $2f$, and $\langle v^3\rangle$ contains three terms varying respectively with f, $2f$, $3f$. We computed the moments of the observed line profiles (see Fig. 6) and performed a frequency analysis in order to compare the observational results to those predicted by the theory. The first moment is the radial velocity. Its analysis is described in a previous section. We found $f = 0.7721$ c/d, $2f$ and $3f$ to be present. In the second moment, we found the frequency 2.3163 c/d $= 3f$ only, while $f = 0.7721$ c/d was found as single frequency in the third moment. We do not obtain the expected frequencies as described above (see also Aerts et al. 1992), so we conclude that the moment variations of HD 105382 are not typical for a standard linear pulsational model.

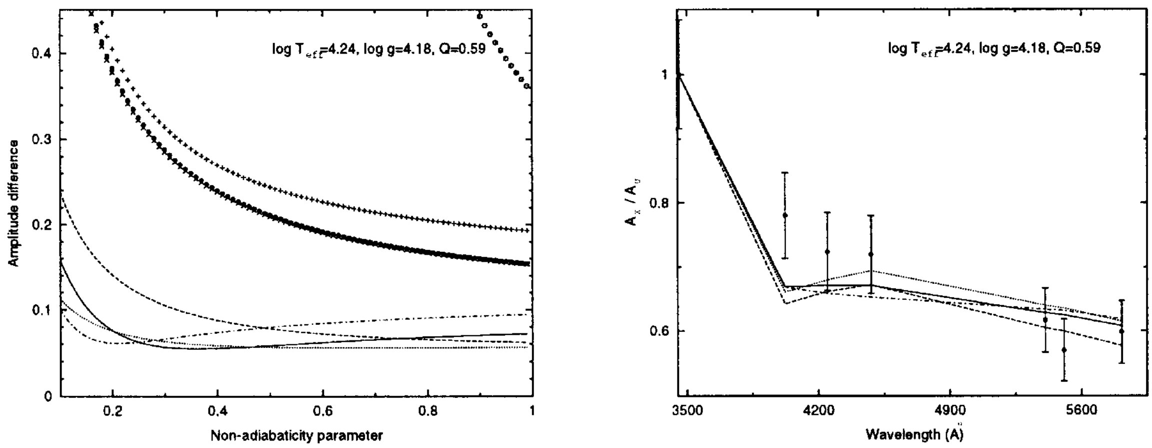

Fig. 5. Left panel: the amplitude difference as a function of the non-adiabaticity parameter S based on the Geneva multicolour photometry: ⊙: $\ell = 0$, dotted line: $\ell = 1$, dashed line: $\ell = 2$, +: $\ell = 3$, full line: $\ell = 4$, ×: $\ell = 5$, dashed-dot line: $\ell = 6$, •: $\ell = 7$. Right panel: the amplitude ratios as a function of wavelength for the four best solutions: dotted line: $\ell = 1$, dashed line: $\ell = 2$, full line: $\ell = 4$, dashed-dot line: $\ell = 6$

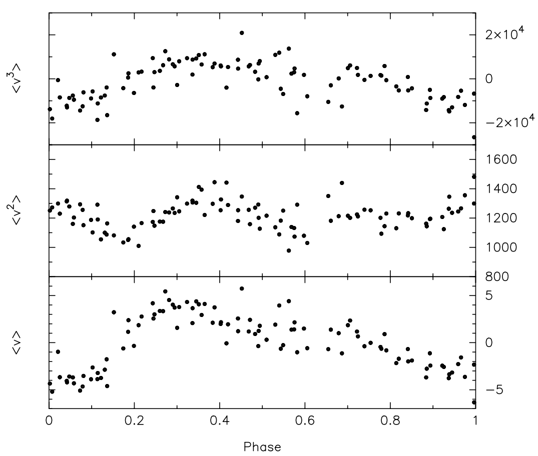

Fig. 6. First three moments of the Si II 4128 Å line

The moment method is the most objective identification criterion at hand in the case of a non-radial pulsator with a slow rotation. Therefore, we have chosen to apply it to our data of HD 105382, despite the fact that a linear description of the first moment is not very accurate. The amplitudes occurring in $\langle v^1\rangle$, $\langle v^2\rangle$, and $\langle v^3\rangle$ depend on the degree ℓ of the pulsation mode, the azimuthal number m, the amplitude of the radial part of the pulsation velocity $v_{\rm p}$, the inclination of the star i, the projected rotational velocity v_Ω and the intrinsic line-profile width σ. Obviously we search for the ℓ and m for which $\langle v^1\rangle$, $\langle v^2\rangle$, and $\langle v^3\rangle$ best fit the observations. To this end, a discriminant is constructed. This discriminant is a function of the differences between the observed and theoretically calculated amplitudes of the first three moments. For each set of wavenumbers (ℓ, m) we determine the values of $v_{\rm p}$, i, v_Ω and σ for which the discriminant $\Gamma_\ell^m(v_{\rm p},\ i,\ v_\Omega,\ \sigma)$ is minimal. Then we chose the mode for which the discriminant attains the lowest value.

To determine the observed amplitudes we fit the observed moments with a sum of varying terms as predicted by the theory, except for the first moment in which we also took into account $2f$ and $3f$. We obtain (see Aerts 1996 for the notation of the different amplitudes and constant):

$$\begin{cases} AA \pm f_{AA} = 3.02 \pm 0.18, \\ DD \pm f_{DD} = 10.2 \pm 12.7, \\ CC \pm f_{CC} = 65.6 \pm 12.8, \\ EE \pm f_{EE} = 1215.8 \pm 8.8, \\ RST \pm f_{RST} = 8043 \pm 774, \\ GG \pm f_{GG} = 3988 \pm 773, \\ FF \pm f_{FF} = 1331 \pm 807. \end{cases}$$

For $\langle v^1\rangle$ we mention that the amplitude of the term varying with $2f$ is 1.6 ± 0.2 km s^{-1} and the one of the term varying with $3f$ is 0.6 ± 0.2 km s^{-1}, which again shows that the variability pattern is non-sinusoidal.

To calculate the theoretical amplitudes we need K, the ratio of the amplitude of the horizontal to the amplitude of the vertical motion in the zero-order rotation approximation:

$$K \simeq 74.437 \left(\frac{M}{M_\odot}\right)\left(\frac{R}{R_\odot}\right)^{-3}\frac{1}{f^2}$$

where M is the mass, R the radius and f the pulsation frequency. We obtain $K = 26$, which means that the transverse component of the velocity field is largely dominant over the radial component.

The outcome of the mode identification with the discriminant is listed in Table 2 for the best solutions in parameter space. We tested ℓ from 0 to 6 because the discriminant is only able to correctly identify modes with low to moderate degree. Since the line-profile variability shown in Fig. 8 does not provide evidence for a large number of moving patterns, the restriction to this degree is fully justified. The other velocity parameters were varied in the

Table 2. The different minima of the discriminant for the Si II 4128 Å line for the best solutions. $v_{\rm p}$ is the amplitude of the radial part of the pulsation velocity, expressed in $\mathrm{km\,s^{-1}}$; i is the inclination angle; v_Ω is the projected rotational velocity, expressed in $\mathrm{km\,s^{-1}}$ and σ is the intrinsic line-profile width, also expressed in $\mathrm{km\,s^{-1}}$

ℓ	m	Γ_ℓ^m	$v_{\rm p}$	i	v_Ω	σ
1	0	0.68	0.3	75°	70	7
5	±1	0.82	0.2	25°	60	15
2	±2	0.84	0.2	15°	70	7
5	±2	0.92	0.1	15°	70	5
3	±2	0.94	0.6	15°	60	11
1	±1	0.99	0.3	25°	70	7
6	±2	1.06	0.5	65°	40	9
⋮	⋮	⋮	⋮	⋮	⋮	⋮

interval $[0.1; 1]$ $\mathrm{km\,s^{-1}}$ for $v_{\rm p}$, $[40; 80]$ $\mathrm{km\,s^{-1}}$ for v_Ω and $[5; 15]$ $\mathrm{km\,s^{-1}}$ for σ.

We find that the more probable mode is (1, 0). We point out that the moment method is not able to distinguish the sign of the azimuthal number. We need to have a second independent check of this result because the moment method is only strictly valid under the assumption of a linear pulsation mode, while the first moment of HD 105382 suggests that non-linear effects may be important in the pulsation.

4.2.2. Mode identification by line-profile fitting

In order to have a second objective way to interpret the line-profile variability in terms of a NRP mode in HD 105382, we used Townsend's (1997) code, called BRUCE, which simulates line profiles for a rotating star undergoing NRP. For a given mode (ℓ, m) the free parameters needed to construct line-profile variations caused by NRP are: the projected rotational velocity v_Ω, the angle of inclination i, the amplitude of the radial part of the pulsation velocity $v_{\rm p}$, the intrinsic line-profile width σ and the initial phase of the mode ϕ.

We want to find the parameters for which the calculated profiles best fit the observed profiles by considering a large grid of possible parameters. In order to keep the computation time feasible, we averaged out all the observed profiles in phase bins of 0.05 of the variability cycle and worked with these 20 averaged observed profiles. They are shown as dotted lines in Fig. 7. As a measure of the goodness of fit we use the standard deviation Σ in the intensity of one wavelength pixel, which was obtained by summing over all wavelength pixels of all 20 profiles. The most likely parameters are those that minimize Σ.

We cover the parameter space by varying the free parameters in the following way: ℓ from 0 to 6, v_Ω from 50 to 80 $\mathrm{km\,s^{-1}}$ with a step 5 $\mathrm{km\,s^{-1}}$, i from 10° to 90° with a step 10°, $v_{\rm p}$ from 2 to 20 $\mathrm{km\,s^{-1}}$ with a step 2 $\mathrm{km\,s^{-1}}$ for non-zonal modes and $v_{\rm p}$ from 0.5 to 1.5 $\mathrm{km\,s^{-1}}$ with a step 0.5 $\mathrm{km\,s^{-1}}$ for modes with $m = 0$, σ from 2.5 to 20 $\mathrm{km\,s^{-1}}$ with a step 2.5 $\mathrm{km\,s^{-1}}$, ϕ from 0 to 0.95 period with a step 0.05 period. The observed profiles are compared to the theoretical profiles and to their orthogonal symmetric profiles in order not to favour a sense of rotation.

The parameters that give the smallest Σ are:

$$\begin{cases} \ell = 4, \\ m = 2, \\ v_\Omega = 65\ \mathrm{km\,s^{-1}} \\ i = 80°, \\ v_p = 4\ \mathrm{km\,s^{-1}}, \\ \sigma = 12.5\ \mathrm{km\,s^{-1}}, \\ K = 5.12, \\ \Sigma = 0.0045 \text{ continuum units.} \end{cases}$$

We note that the contribution due to geometric effects to the magnitude amplitude is 0.003, which is an order of magnitude smaller than the observed one. The fit for these parameters is shown in Fig. 7. We see that the best NRP model is not able to explain the line-profile variations in a detailed way.

In order to test whether the assumption of an intrinsic Gaussian is too restrictive, we also used theoretical intrinsic profiles kindly provided by Dr. T. Rivinius. These are constructed using the atmospheric code ATLAS 9 and BHT (see Gummersbach et al. 1998) and fixing the microturbulence at 2 $\mathrm{km\,s^{-1}}$. We took into account temperature effects for the adiabatic case and the non-adiabatic case by introducing two extra parameters which are temperature amplitude and phase. We did not find a better fit with such more realistic intrinsic profile and temperature effects. We note that the same model as above with temperature effects leads to amplitudes in U, B and V filters of about 0.01, which is compatible with the photometric measurements. We also allowed the observed period to be negative. Again, we did not obtain a better result.

5. Rotational modulation model

In order to confront the observations with a rotational modulation model we used a code kindly put at our disposal by Dr. L. Balona. This code calculates line-profile variations for a spotted star. For simplicity, we only considered one spot.

The following parameters are needed to construct line-profile variations caused by a circular spot: the equatorial and polar radii $R_{\rm e}$ and $R_{\rm p}$, the equatorial and polar fluxes $F_{\rm e}$ and $F_{\rm p}$, the projected rotational velocity v_Ω, the angle of inclination i, the linear limb-darkening coefficient u, the intrinsic line-profile width in the photosphere $\sigma_{\rm i}$, the longitude (relative to some arbitrary epoch) λ, the latitude β, the spot radius in degrees γ, the flux from the spot relative to the photosphere F, the intrinsic line-profile width in the spot $\sigma_{\rm s}$.

We again determine the parameters for which the theoretical profiles best fit the observations by minimizing the standard deviation Σ in the intensity over all profiles as done for BRUCE. We take $R_{\rm e} = R_{\rm p} = 3\ R_\odot$, $F_{\rm e} = F_{\rm p} = 1$ and $u = 0.36$. The other eight parameters are free. We point out that the NRP model also contains eight free parameters.

We cover the parameter space by varying the free parameters in the following way: λ from 10° to 90° with a step 10°, β from −90° to 90° with a step 10°, γ from 30° to 50° with a step 10°. To simulate a spot in the three other quarters, the observed profiles are shifted by 0.25, 0.5 and 0.75 period. We take F from 0.8 to 1.2 with a step 0.1. v_Ω is taken from 60 to 80 $\mathrm{km\,s^{-1}}$ with a step 5 $\mathrm{km\,s^{-1}}$. Obviously both senses of rotation are envisaged. As we adopt the radius of the star $R = 3\ R_\odot$ and the frequency of rotation $f = 0.7721$ c/d, for each adopted v_Ω, i is fixed. However, as the value of the radius is not certain, we consider the values of i corresponding to a radius of 3, 4, 5, 6 $R_\odot$. The tested values of σ depend on the adopted value of v_Ω. For $v_\Omega = 60\ \mathrm{km\,s^{-1}}$, we take $\sigma = 12.5$, 15, 17.5, 20, 22.5 $\mathrm{km\,s^{-1}}$; for $v_\Omega = 65\ \mathrm{km\,s^{-1}}$, $\sigma = 10$, 12.5, 15, 17.5, 20 $\mathrm{km\,s^{-1}}$; for $v_\Omega = 70\ \mathrm{km\,s^{-1}}$, $\sigma = 7.5$, 10, 12.5, 15, 17.5 $\mathrm{km\,s^{-1}}$; for $v_\Omega = 75\ \mathrm{km\,s^{-1}}$, $\sigma = 5$, 7.5, 10, 12.5, 15 $\mathrm{km\,s^{-1}}$ and for $v_\Omega = 80\ \mathrm{km\,s^{-1}}$, $\sigma = 2.5$, 5, 7.5, 10, 12.5 $\mathrm{km\,s^{-1}}$.

We also constrained the calculated light amplitude so that this corresponds to the observed one. The parameters that give the smallest Σ are:

$$\begin{cases} \lambda = 50^\circ, \\ \beta = 20^\circ, \\ \gamma = 40^\circ, \\ F = 1.1, \\ v_\Omega = 65\ \mathrm{km\,s^{-1}}, \\ i = 34^\circ, \\ \sigma_i = 15\ \mathrm{km\,s^{-1}}, \\ \sigma_s = 12.5\ \mathrm{km\,s^{-1}}, \\ \Sigma = 0.0032 \text{ continuum units.} \end{cases}$$

For this model the magnitude amplitude is 0.017. The fit for these parameters is shown in Fig. 7. The best spot model is not able either to explain the line-profile variations satisfactorily. We recall, however, that we have limited our modeling to one spot. Allowing more than one spot would increase the number of free parameters and would yield unrealistic computation times.

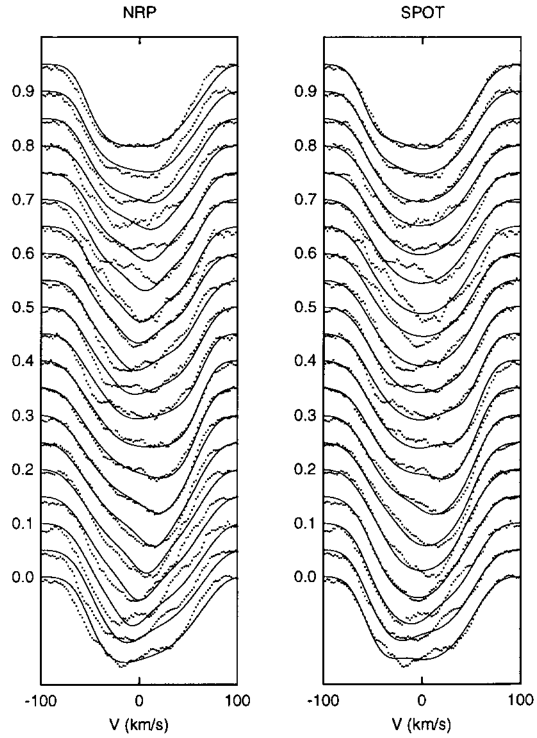

Fig. 7. Observed line profiles of the Si II 4128 Å line (dots) averaged over phase bins of 0.05 and theoretical line profiles (full lines) for 1) left: the NRP model with $(\ell, m) = (4, 2)$, 2) right: the spot model with one spot

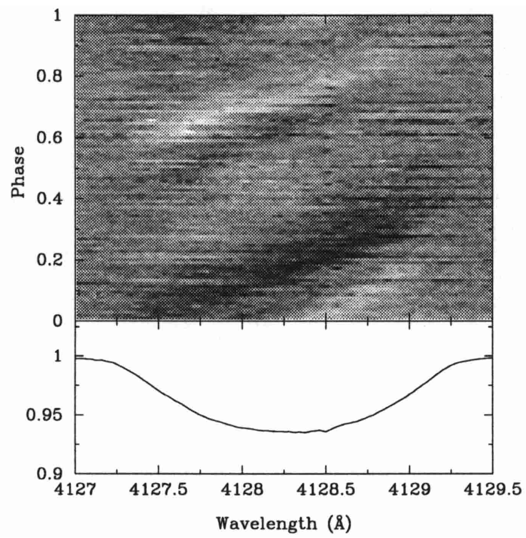

Fig. 8. The 105 residual spectra with respect to the average line profile of the Si II 4128 Å line as a function of the phase

6. The nature of the low-level subfeatures

The residual spectra with respect to the average line profile of the Si II 4128 Å line are represented as a function of the phase (calculated for the frequency 0.7721 c/d) in a grey-scale picture (see Fig. 8). Black denotes local absorption while white represents local emission. It can be noted that a large subfeature is traversing the profile from blue to red during the first part of the cycle. The motion during the second part is less clear.

In Fig. 7 we can see a large number of subfeatures in the observed line profiles of the Si II 4128 Å line. In order to know if these subfeatures are noise or are real we subtracted the average profile from each profile and we looked for bumps. We succeeded to follow the big absorption bump corresponding to the phase interval [0; 0.4] in Fig. 8 as well as the emission bump seen in the same figure for the phases [0.6; 0.8]. No other bump with a systematic trend in phase is visible in Fig. 8 and so we conclude that the low-level subfeatures cannot be distinguished from noise on the basis of our data.

7. Conclusions

We have made an extensive study of the B 6 III star HD 105382 by means of multicolour photometry and high-resolution spectroscopy spread over respectively one and two years. We provide evidence that this star is misclassified as a Be star. All the data point out that there is only one period of 1.295 days present in the star. We confronted the line-profile variations with both a non-radial pulsation model and with a spot model using the light amplitude as a constraint. The latter model gives a slightly better explanation for the line-profile variations in the case of a single spot, but the difference between the rivalling hypotheses is only marginal. In fact, none of the two models is able to explain the variability in a satisfactory way. We therefore derive at the same conclusion as for the Be line-profile variable 28 CMa: there is no consensus about the best explanation for the variability, even in this case of a "simple" monoperiodic star that does not exhibit long-term trends. We are thus left with the question-mark in the title of our paper. The true nature of HD 105382 remains a puzzle, which can only be solved by a much more dedicated campaign of high-resolution spectroscopy spread over several years.

Two other periodically variable B-type stars discovered from Hipparcos behave similarly: HD 138769, which is classified as a B 3 IV p star and has also one dominant mode, and HD 131120 which is a B 7 II/III star. The latter object was classified as a slowly pulsating B star by Waelkens et al. (1998), but Aerts et al. (1999b) find only one dominant period in the photometry and in the spectroscopy and the radial-velocity curve is clearly non-sinusoidal. We will elaborate on these two objects in the near future in order to compare their variability with the one exhibited by HD 105382.

Acknowledgements. We are grateful to Dr. Thomas Rivinius for pointing out that the Hα spectrum published by Aerts (2000) resembles the one of δ Cen. This helped us to conclude that probably all previous reports of the Be nature of HD 105382 are based upon the same mistake. We thank an anonymous referee for the valuable comments which help us in improving this paper. This work was supported by the P.A.I. (Pôle d'Attraction Interuniversitaire).

References

Aerts, C., De Pauw, M., & Waelkens, C. 1992, A&A, 266, 294
Aerts, C. 1996, A&A, 314, 115
Aerts, C., De Boeck, I., Malfait, K., & De Cat, P. 1999a, A&A, 347, 524
Aerts, C., De Cat, P., Peeters, E., et al. 1999b, A&A, 343, 872
Aerts, C. 2000, in The Be phenomenon in Early-Type Stars, ed. M. A. Smith, H. F. Henrichs, & J. Fabregat, PASP, Conf. Ser., in press
Baade, D., & Balona, L. A. 1994, in IAU Symposium 162: Periodic variability of Be stars: non-radial pulsation or rotational modulation?, ed. L. A. Balona, et al. (Kluwer Academic Publishers), 311
Balona, L. A. 1995, MNRAS, 277, 1547
Balona, L. A., Aerts, C., & Stefl, S. 1999, MNRAS, 305, 519
Claria, J. J., & Escosteguy, L. A. 1981, PASP, 93, 636
Dachs, J., et al. 1981, A&AS, 43, 427
De Cat, P., Aerts, C., De Ridder, J., et al. 2000, A&A, 355, 1015
Flower, P. J. 1996, ApJ, 469, 355
Gummersbach, C. A., Kaufer, A., Schäfer, D. R., Szeifert, T., & Wolf, B. 1998, A&A, 338, 881
Heynderickx, D., Waelkens, C., & Smeyers, P. 1994, A&AS, 105, 447
Hiltner, W. A., Garrison, R. F., & Schild R. E. 1969, ApJ, 157, 313
Künzli, M., North, P., Kurucz, R. L., & Nicolet, B. 1997, A&AS, 122, 51
Kurucz, R. L. 1979, ApJS, 40, 1
Maintz, M., Rivinius, T., Tubbesing, S., et al., in The Be phenomenon in Early-Type Stars, ed. M. A. Smith, H. F. Henrichs, & J. Fabregat, PASP, Conf. Ser., in press
Rivinius, T., Baade, D., Stefl, S., et al. 1998, A&A, 336, 177
Pamyatnykh, A. A. 1999, Acta Astron., 49, 119
Roberts, D. H., Lehár, J., & Dreher, J. W. 1987, AJ, 93, 968
SAS/ User's Guide 1990, Version 6, volume 1–2, SAS Institute Inc., Cary, NC
Schaller, G., Schaerer, D., Meynet, G., & Maeder, A. 1992, A&AS, 96, 269
Slettebak, A., Collins, G. W., II, Parkinson, T. D., et al. 1975, ApJS, 29, 137
Stamford, P.A., & Watson, R. D. 1981, Ap&SS, 77, 131
Stellingwerf, R. F. 1978, ApJ, 224, 953
Townsend, R. H. D. 1997, MNRAS, 284, 839
Wade, R. A., & Rucinski, S. M. 1985, A&AS, 60, 471
Waelkens, C., Aerts, C., Kestens, E., et al. 1998, A&A, 330, 215